

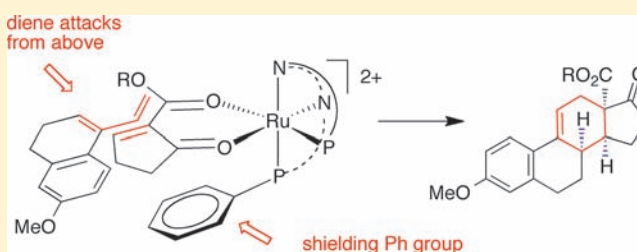
Asymmetric Diels–Alder and Ficini Reactions with Alkylidene β -Ketoesters Catalyzed by Chiral Ruthenium PNNP Complexes: Mechanistic Insight

Christoph Schotes, Martin Althaus, Raphael Aardoom, and Antonio Mezzetti*

Department of Chemistry and Applied Biosciences, ETH Zürich, CH-8093 Zürich, Switzerland

S Supporting Information

ABSTRACT: Hydride abstraction from the β -position of the enolato ligand of the previously reported complex $[\text{Ru}(\mathbf{3a-H})(\text{PNNP})]\text{PF}_6$ ($\mathbf{5a}$; $\mathbf{3a-H}$ is the enolate of 2-*tert*-butoxycarbonylcyclopentanone) with $(\text{Ph}_3\text{C})\text{PF}_6$ gives the dicationic complex $[\text{Ru}(\mathbf{6a})(\text{PNNP})]^{2+}$ ($\mathbf{7a}$) as a single diastereoisomer, which contains the unsaturated β -ketoester 2-*tert*-butoxycarbonyl-2-cyclopenten-1-one ($\mathbf{6a}$) as a chelating ligand. The methyl analogue 2-methoxycarbonylcyclopentanone ($\mathbf{3b}$) gives $[\text{Ru}(\mathbf{3b-H})(\text{PNNP})]\text{PF}_6$ as a mixture of noninterconverting diastereoisomers (ester group of $\mathbf{3b}$ trans to P, $\mathbf{5b}$; or to N, $\mathbf{5c}$), which were separated by column chromatography. Hydride abstraction from $\mathbf{5b}$ (or $\mathbf{5c}$) yields diastereomerically pure $[\text{Ru}(\mathbf{6b})(\text{PNNP})]^{2+}$ ($\mathbf{7b}$ or $\mathbf{7c}$). Complexes $\mathbf{7b}$ and $\mathbf{7c}$ do not interconvert at room temperature in CD_2Cl_2 and form opposite enantiomers of the Diels–Alder adduct upon reaction with Dane’s diene (1 equiv). X-ray studies of $\mathbf{7a}$, $\mathbf{5b}$, and $\mathbf{5c}$ give insight into the origin of enantioselection and the sense of asymmetric induction in the previously reported asymmetric Diels–Alder and Ficini cycloaddition reactions with 2,3-disubstituted butadienes and ynamides, respectively. Stoichiometric reactions (substrate coordination, cycloaddition, and product displacement) between $[\text{Ru}(\text{OEt}_2)_2(\text{PNNP})]^{2+}$ ($\mathbf{2}$), $\mathbf{6b}$ (or $\mathbf{6a}$), and Dane’s diene ($\mathbf{15}$, to give estrone derivatives) or *N*-benzyl-*N*-(cyclohexylethynyl)-4-methylbenzenesulfonamide ($\mathbf{17}$, to give cyclobutenamides) suggest that product displacement from the catalyst is turnover limiting.



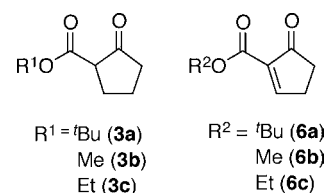
INTRODUCTION

Enantioselective Diels–Alder reactions have witnessed tremendous advances in the last 20 years,¹ but the restricted scope of dienophiles, limited mechanistic understanding, and lack of reliable stereochemical models with most catalysts are still open challenges.² Thus, although the breadth of the substrate scope in enantioselective Diels–Alder reactions has considerably increased recently^{1e} driven by Corey’s chiral cationic oxazaborolidine catalysts,^{1a,3} acrolein derivatives and unsaturated imides are still the most commonly used dienophiles. In contrast, poor dienophiles such as α -methylene β -ketoesters have been rarely studied in asymmetric Diels–Alder reactions,⁴ probably because the Lewis acidity of most chiral catalysts is too low for systems whose intrinsic reactivity (that is, for the uncatalyzed, thermal reaction) is marginal.³

Additionally, bulky unsaturated β -ketoesters, such as the even less reactive cyclic carboxypentenones, are challenging Diels–Alder substrates, as they tend to polymerize⁵ and give keto–enol tautomerization.⁶ Therefore, the corresponding tetrahydro-1-indanones are formed in low yield and under harsh conditions⁵ unless elaborate protocols are used.⁷ Overall, alkylidene β -ketoesters have been rarely used also in other asymmetric catalytic reactions, and some applications in enantioselective conjugate addition reactions have appeared only recently.⁸

Our interest in alkylidene β -ketoesters has developed from the study of the coordination of their saturated analogues, such as 2-*tert*-butoxycarbonylcyclopentanone ($\mathbf{3a}$) (Chart 1), to the

Chart 1

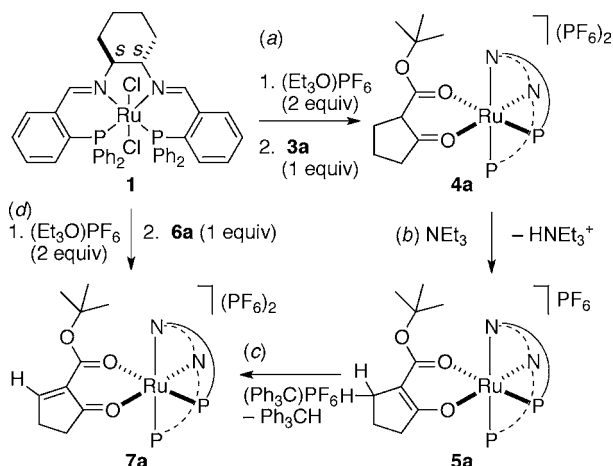


highly oxophilic ruthenium/PNNP fragment.^{9,10} Double chloride abstraction from the dichloro complex¹¹ $[\text{RuCl}_2(\text{PNNP})]$ ($\mathbf{1}$) gives an elusive species that we tentatively formulate as $[\text{Ru}(\text{OEt}_2)_2(\text{PNNP})](\text{PF}_6)_2$ ($\mathbf{2}$),⁹ which reacts with saturated β -ketoesters such as 2-*tert*-butoxycarbonylcyclopentanone ($\mathbf{3a}$) to give $[\text{Ru}(\mathbf{3a})(\text{PNNP})](\text{PF}_6)_2$ ($\mathbf{4a}$) (Scheme 1a). The dicationic β -ketoester adducts of type $\mathbf{4}$ offer a rare example of the coordination of a 1,3-dicarbonyl compound in its neutral, non-enolized form¹² and are intermediates in highly enantioselective C–C and C–heteroatom bond forming reactions of saturated β -ketoesters, such as Michael addition,^{12a,b} hydroxylation,¹³ and fluorination.¹⁴

The enhancement of the acidity of the β -ketoester upon coordination to the dicationic ruthenium PNNP fragment plays a pivotal role in these reactions, and complexes of type $\mathbf{4}$ are

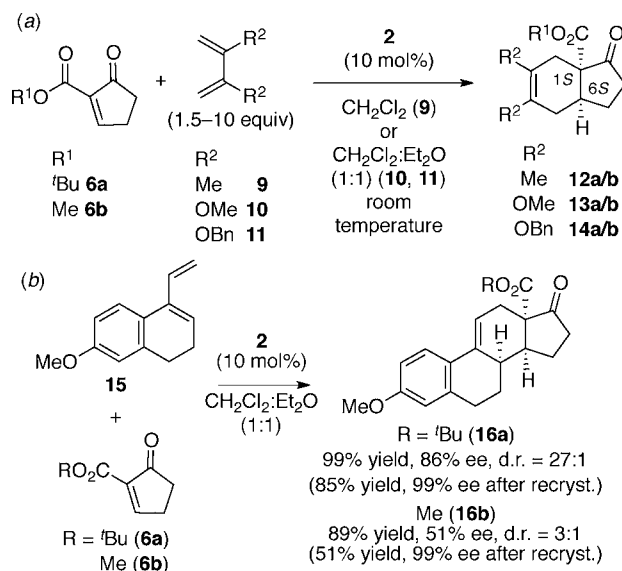
Received: November 4, 2011

Published: December 19, 2011

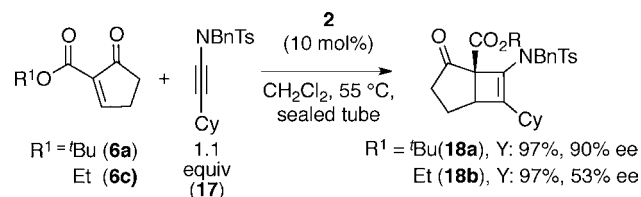
Scheme 1. Synthesis of β -Ketoester Complexes

easily deprotonated to the enolato analogues **5** (Scheme 1b).^{9,12,14} Recently, we serendipitously discovered that the enolato ligand (**3a-H**) in $[\text{Ru}(\mathbf{3a-H})(\text{PNNP})]\text{PF}_6$ (**5a**) undergoes β -hydride abstraction when treated with trityl hexafluorophosphate (Scheme 1c). The resulting unsaturated β -ketoester *2-tert*-butoxycarbonyl-2-cyclopenten-1-one (**6a**) remains coordinated to ruthenium in the well-defined adduct $[\text{Ru}(\mathbf{6a})(\text{PNNP})]^{2+}$ (**7a**). Alternatively, **7a** can be prepared from $[\text{Ru}(\text{OEt})_2(\text{PNNP})](\text{PF}_6)_2$ (**2**) and **6a** (Scheme 1d), and analogous complexes are obtained with other 2-alkyloxycarbonyl-2-cyclopenten-1-ones (Chart 1). We recently described the use of these species as catalysts for the highly enantioselective cycloaddition reactions with dienes (Diels–Alder)¹⁵ and ynamides (Ficini reaction)¹⁶ in two preliminary reports (see Schemes 2 and 3).

Scheme 2. Asymmetric Diels–Alder Reaction with Substituted 2,3-Butadienes



To the best of our knowledge, these are the first enantioselective cycloaddition reactions that use cyclic unsaturated β -ketoesters to give highly enantiomerically enriched molecules. Such products bear a quaternary all-carbon stereocenter at the bridgehead position of a bicyclic system and have potential biological interest.¹⁵ Additionally, although structural information

Scheme 3. Asymmetric Ficini Reaction^a

^aFor 11 other examples with different ynamides, see ref 16.

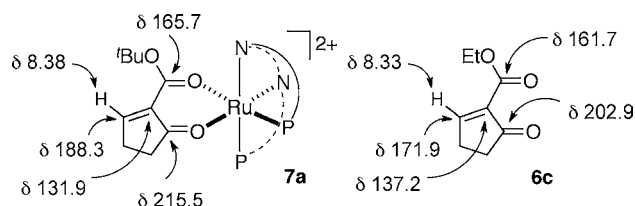
concerning the substrate/catalyst adduct is deemed to be pivotal to mechanistic understanding, and the key to the broad applicability of a Diels–Alder catalyst,² such structurally characterized adducts as **7a** are rare. In the specific case of alkylidene β -ketoesters, the closest analogues are the copper-catalyzed Michael reactions of alkylidene malonates¹⁷ and the iridium-promoted Nazarov cyclization of divinyl ketones.^{18,19} We show herein that the structures of the catalyst adduct **7a** with the unsaturated β -ketoester **6a** and some related species give valuable insight into the mechanistic details of the Diels–Alder and [2 + 2] cycloaddition reactions.

RESULTS AND DISCUSSION

Hydride Abstraction from Enolato Complex 5a. We discovered the hydride abstraction reaction in Scheme 1c while studying the possible involvement of a ruthenium(III) species in the electrophilic fluorination of **3a** with catalyst **2**.^{12c,14,20} Thus, the Ru(II) enolato complex $[\text{Ru}(\mathbf{3a-H})(\text{PNNP})]\text{PF}_6$ (**5a**) was treated with a number of one-electron oxidants, in particular $(\text{NH}_4)_2[\text{Ce}(\text{NO}_3)_6]$ (CAN), $\text{K}_2\text{S}_2\text{O}_8$ (in the presence of 18-crown-6), AgPF_6 , and $(\text{Ph}_3\text{C})\text{PF}_6$ in CD_2Cl_2 . Cerium(IV) ammonium nitrate and potassium persulfate did not react under these conditions. Instead, AgPF_6 gave a mixture of diamagnetic products whose major component (46%) was the unsaturated β -ketoester complex **7a**, which we were not able to identify at this stage. In all experiments, the ¹H and ³¹P NMR spectra of the reaction solutions were sharp and furnished no evidence of paramagnetic species being formed. Eventually, we discovered that $(\text{Ph}_3\text{C})\text{PF}_6$ (1 equiv) reacts with **5a** in CD_2Cl_2 within seconds, as indicated by a color change from orange to yellow. The ³¹P NMR spectrum of the reaction solution showed quantitative conversion of **5a**, and the only observable product featured an AX pattern at δ 63.2 and δ 50.4 ($J_{\text{P,P}'} = 29.3$ Hz). The ¹H NMR spectrum showed the characteristic signal for the tertiary C–H hydrogen in Ph_3CH (δ 5.59) and a doublet of doublets at δ 8.38 for the vinylic proton of the coordinated α -alkylidene β -ketoester, which indicated that a hydride abstraction at the β -position of the coordinated deprotonated β -ketoester **3a** had occurred (Scheme 1c).

Accordingly, the ¹³C NMR spectrum of the reaction solution exhibited signals at δ 131.9 and 188.3 that we assign to the sp² carbon atoms of the newly formed double bond. The vinylic proton at δ 8.38 shows correlation cross-peaks to the keto carbonyl carbon at δ 215.5 and to the ester carbonyl C atom at δ 165.7 in the long-range ¹³C,¹H-HMQC NMR spectrum (Chart 2, left). Thus, we formulate the product of the reaction as the dicationic complex $[\text{Ru}(\mathbf{6a})(\text{PNNP})]^{2+}$, in which the enolato ligand in complex **5a** has been transformed into the unsaturated β -ketoester **6a**. The ¹³C NMR signal of the olefin carbon atom is shifted considerably toward higher frequency compared with a related free enone ester (δ 188.3 vs 171.9, Chart 2, right). Thus, the coordination to ruthenium enhances

Chart 2



the polarization of the C=C double bond by withdrawing electron density from the β -carbon atom of the coordinated enone **6a**.²¹ The resulting stabilization of the corresponding LUMO improves the interaction with the HOMO of electron-rich dienes in Diels–Alder reactions²² and enhances the reactivity of the C=C double bond toward the cycloaddition reactions discussed below.

Both the ^1H and ^{31}P NMR spectrum show that the hydride abstraction is quantitative and well behaved, as no side-products (apart from Ph_3CH) are detected. The triphenylcarbenium ion (tritylium cation) reacts with **5a** as a hydride abstractor and hence as a two-electron oxidant to give triphenylmethane²³ instead of being reduced by one electron to the trityl radical and dimerizing to Gomberg's dimer.²⁴ The hydride-abstracting properties of tritylium salts have been used in organic reactions, for instance for the conversion of secondary alcohols to ketones.²⁵ The trityl cation is known to abstract a hydride from silyl enol ethers to give the corresponding enones²⁶ and has been used in transition metal chemistry for hydride abstraction reactions from alkyl ligands to give carbene complexes,²⁷ but its reaction with an enolato complex (and β -ketoesters in general) is, to the best of our knowledge, unprecedented.

The closest literature analogue of enolate oxidation (Scheme 1c) is the oxidative cleavage of titanium bound enediolates by triphosgene to form cyclopentane-1,2-diones, a reaction whose mechanism has not been investigated.²⁸ Apart from the general selenide oxidation–elimination reaction,²⁹ the oxidation of β -ketoesters to their unsaturated analogues has been achieved with a combination of $\text{Cu}(\text{OAc})_2$ and $\text{Pb}(\text{OAc})_4$ ³⁰ or with 2,3-dichloro-5,6-dicyanobenzoquinone (DDQ).³¹ These methods make use of highly toxic primary oxidants and often suffer from moderate yields and narrow substrate scope. Therefore, the tandem deprotonation/hydride abstraction reaction described above is an elegant and clean preparation of unsaturated β -ketoesters on a small scale. We show below that, beyond fundamental aspects, this approach is chemically useful for the in situ preparation of pure catalysts.

cis- β -[Ru(6a)(PNNP)]²⁺ (7a). Complex **7a** was independently prepared by adding 2-*tert*-butoxycarbonyl-2-cyclopenten-1-one (**6a**) to a CD_2Cl_2 solution of freshly prepared $[\text{Ru}(\text{OEt})_2(\text{PNNP})](\text{PF}_6)_2$ (**2**) (Scheme 1d). The reaction is complete within 15 min, as indicated by a slight color change of the reaction solution from reddish-brown to orange-red. The ^{31}P NMR spectrum of the reaction solution shows the AX pattern of **7a** as the only identifiable product. However, small impurities (<2% of total integrated intensity) indicate that this synthetic pathway is less clean than the hydride abstraction (Scheme 1a–c). Attempts to prepare **7a** by the latter route on a larger scale (50–100 mg) by precipitation with hexane from the CD_2Cl_2 reaction solution led to extensive decomposition. A similar behavior has been observed for the saturated analogue **4a**,^{12a} which is not surprising in view of the labile nature of the

coordination bond between ruthenium and a neutral oxygen donor (see below). Nonetheless, we were able to grow crystals of (*rac*)-**7a**.

X-ray Crystal Structure of Complex (*rac*)-7a. Complex (*rac*)-**7a** was prepared by treating the enolato complex (*rac*)-**5a** (containing the (*R,R*),(*S,S*)-PNNP ligand) with $(\text{Ph}_3\text{C})\text{PF}_6$ (1 equiv) in CD_2Cl_2 . Layering the solution directly after the reaction in an NMR tube with *n*-hexane gave single crystals of the centrosymmetric triclinic space group $\text{P}\bar{1}$, whose asymmetric unit contains one complex molecule, two $[\text{PF}_6]^-$ anions, and two CD_2Cl_2 molecules. Figure 1 shows an ORTEP drawing

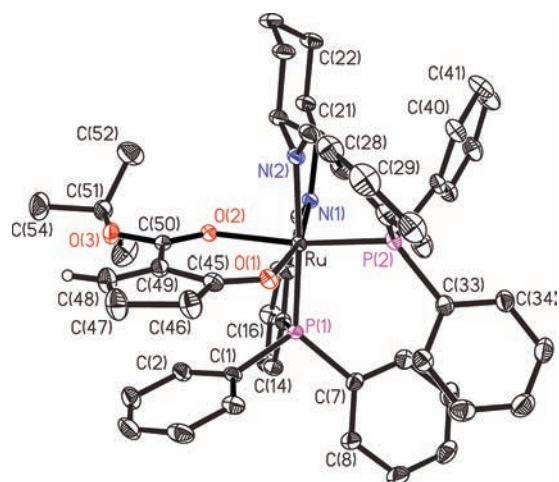


Figure 1. ORTEP drawing of (OC-6-42-A-(*S,S*))-**7a** (ellipsoids at 30% probability).

of the complex with the (*S,S*)-PNNP ligand, which is the enantiomer used in all catalytic reactions discussed below.

The coordination sphere of ruthenium is a distorted octahedron with the absolute configuration OC-6-42-A.³² The (*S,S*)-PNNP ligand is arranged in the Λ -*cis*- β mode and in a conformation that is very similar to those observed in the related enolato complex **5a** and in the β -keto acid complex $[\text{Ru}(3a\text{-}^t\text{Bu})(\text{PNNP})]^{2+}$ (**8**) (**3a-^tBu** is the acid obtained by hydrolysis of the $^t\text{BuOC}(\text{O})$ ester group of **3a**).^{12a,33} The unsaturated β -ketoester **6a** binds with the keto oxygen O(1) trans to N(1) and with the ester carbonyl oxygen O(2) trans to P(2), as in the enolato complex **5a**, which suggests that the hydride abstraction does not cause a major structural rearrangement. The Ru–O(1) distance (trans to N) is significantly shorter than Ru–O(2) (trans to P) (2.107(2) vs 2.172(2) Å), as observed in **8**,^{12a} and reflects the lower trans influence of the imino donor as compared to phosphine (Table 1).

The C–C and C–O bond distances in the coordinated enone ester differ only marginally from average values (Chart 3).³⁴ The conjugation between the C(48)–C(49) double bond and the carbonyl groups in **7a**, whose effect on the ^{13}C NMR chemical shift of C(48) has been discussed above, does not significantly affect the C–O distance in the keto group, as indicated by the comparison with the closest analogue, the saturated acid complex **8**.^{12a} The comparison between **5a** and **7a** shows the expected differences between an enolato and an enone ligand, that is, the shortening of the C(48)–C(49) bond from single to double, the lengthening of the C(45)–C(49) distance (by 0.08 Å), and the shortening of the carbonyl O(1)–C(45) bond. The effect is smaller for the O(2)–C(50) bond, as

Table 1. Selected Distances (Å) of 5a, 7a, 5b, and 5c (see also Chart 3)

	7a	5a	5b	5c
Ru–P(1)	2.2973(8)	2.2803(8)	2.2820(7)	2.280(2)
Ru–P(2)	2.2692(8)	2.2681(8)	2.2601(6)	2.277(2)
Ru–N(1)	2.047(3)	2.044(2)	2.050(2)	2.030(5)
Ru–N(2)	2.083(3)	2.097(3)	2.091(2)	2.072(5)
Ru–O(1)	2.107(2)	2.082(2)	2.086(2)	2.108(4)
Ru–O(2)	2.172(2)	2.144(2)	2.128(2)	2.109(4)
C(1)⋯C(49)	3.471(4)	3.554(5)	3.572(4)	3.47(1)
C(4)⋯C(48)	3.760(1)	4.058(5)	4.047(4)	3.78(1)
P(1)–Ru–C(49)	91.27(5)	92.52(6)	94.85(5)	92.5(1)
C(49)⋯Ru–P(1)–C(1)	–8.3(1)	–12.0(1)	–11.4(1)	–4.9(3)

Chart 3

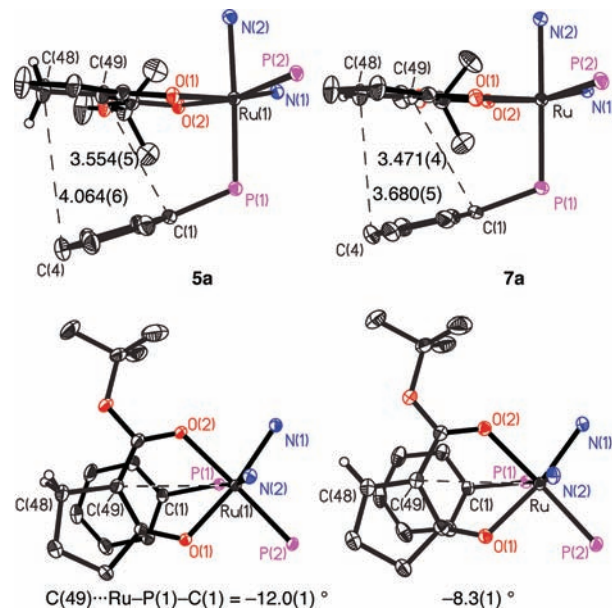
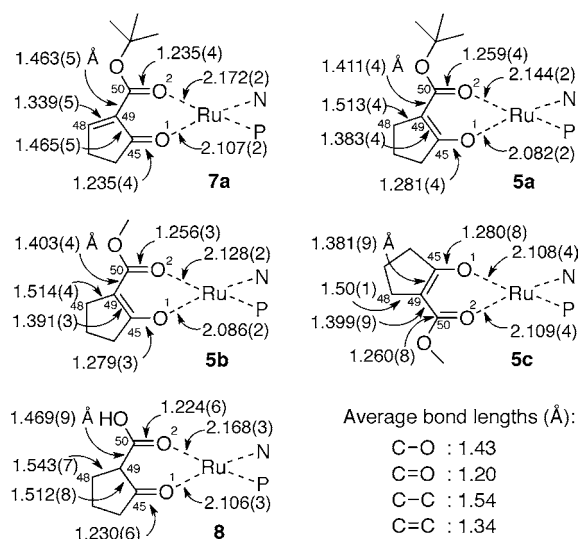


Figure 2. Partial ORTEP views of 5a and 7a (the PNNP framework is omitted for clarity, except for the C(1)–C(6) phenyl) (distances in angstroms). The angles between the C(1)–C(6) phenyl ring and the C(45)–C(49)–C(50) plane are 23.3(4) and 14.0(4)°, respectively.

the ester moiety is less enolized than the ketone carbonyl^{12a} and, therefore, gains less double bond character upon hydride abstraction. The Ru–P and Ru–N distances in 7a and in the enolato complex 5a are very similar (Table 1). However, the Ru–O distances are slightly longer in 7a than in 5a, which reflects the weaker coordination of the neutral unsaturated β -ketoester in 7a as compared to the anionic enolato ligand in 5a.

Interesting changes on going from the enolato complex 5a to the enone derivative 7a are the shrinking of the C(1)⋯C(49) and C(4)⋯C(48) nonbonding contacts and of the C(49)⋯Ru–P(1)–C(1) torsion angle (Figure 2). Also, the dihedral angle between the plane defined by C45/C49/C50 of the β -ketoester and that of the shielding phenyl ring is reduced from 23.3° to 14.0°.³⁵ These changes indicate enhanced π – π interactions between the C(1)–C(6) phenyl ring and the β -ketoester in 7a as compared to 5a and reflect the higher π -acidity of the electron-poor enone moiety in comparison to the enolato ligand. Hence, the two ring systems align and move closer together in 7a. Interestingly, Corey has proposed that the π – π stacking between aromatic groups of the catalyst and acrolein- or enone-type substrates in the transition state directs the enantioselectivity of cationic oxazaborolidine catalysts,^{1a,3} but, to the best of our knowledge, the effect has never been visualized by X-ray crystallography of a substrate/catalyst adduct.

Catalytic Diels–Alder Reaction. As described in a preliminary report,¹⁵ the dicationic derivative [Ru(OEt)₂(PNNP)](PF₆)₂ (**2**) catalyzes the enantioselective Diels–Alder reaction of the unsaturated β -ketoesters **6** with 2,3-dimethylbutadiene

(**9**), 2,3-dimethoxybutadiene (**10**), and 2,3-(dibenzoyloxy)butadiene (**11**) (Scheme 2a). The corresponding alkoxy-carbonyl-tetrahydro-1-indanones **12–14** are formed at room temperature overnight with up to 93% ee (Table 2). With Dane's diene (**15**), the estrone derivative (8*R*,13*S*,14*S*)-13-*tert*-butoxycarbonyl-3-methoxy-7,8,12,13,15,16-hexahydro-6*H*-cyclopenta[*a*]phenanthren-17(14*H*)-one (**16a**) was quantitatively obtained with 86% ee or as a single enantiomer after recrystallization (Scheme 2b). Of the two diastereoisomers (ester-*exo* and ester-*endo*) that are possible with **15**, the ester-*exo* product is favored, but the diastereomeric ratio strongly depends on the ester moiety and drops from 27:1 for the *tert*-butyl ester **6a** to 3:1 for the methyl analogue **6b** (before recrystallization).

Under optimized conditions, the reaction with activated dienes such as **15** gives essentially quantitative yields with a nearly stoichiometric amount of the reagent, whereas 2,3-dimethylbutadiene (**9**) has to be used in excess (10 equiv). Except for the reaction with **9**, a CH₂Cl₂:Et₂O (1:1) solvent mixture was required to achieve high yields in a reproducible fashion. Also, high enantioselectivity was only obtained with the bulky unsaturated β -ketoester **6a** (Table 2, entries 4, 5). These effects are discussed and explained in the context of the stoichiometric reactions described below.

Table 2. Asymmetric Diels–Alder Reaction of 6a and 6b with Various Dienes^a

entry	dienophile	diene	product	R ¹	R ²	yield (%)	ee (%)
1 ^b	6a	9 ^c	12a	^t Bu	Me	82	67
2	6a	9 ^c	12a	^t Bu	Me	67	67
3	6a	10	13a	^t Bu	OMe	86	64
4	6a	11	14a	^t Bu	OBn	91	93
5	6a	15	16a	^t Bu		99	86
6 ^b	6b	9 ^c	12b	Me	Me	88	69
7	6b	9 ^c	12b	Me	Me	52	84
8	6b	10	13b	Me	OMe	62	66
9	6b	11	14b	Me	OBn	90	76
10	6b	15	16b	Me		89	51

^aFrom ref 15, **2** (10 mol %) as catalyst, room temperature, in CH₂Cl₂/Et₂O (1:1) (unless otherwise stated). ^bIn pure CH₂Cl₂. ^c10 equiv.

As discussed above, the coordination of the alkylidene β -ketoester **6** to the Ru/PNNP fragment in the adducts of type **7** (Scheme 1d) lowers the energy of the LUMO and activates the substrate toward cycloaddition of electron-rich dienes. The stereochemical course of the reaction was determined with the unsymmetrical diene **15** by reduction of the carbonyl moiety of its Diels–Alder adduct **16a**, esterification with (–)-camphanic acid chloride, and X-ray structure determination.^{15a} The absolute configuration of **16a** (8*R*,13*S*,14*S*) indicates that the diene **15** approaches the metal-bound substrate over the less hindered cyclopentenone ring. In the pericyclic transition state, the ester residue points away from the forming ring and the ester-*exo* product is formed (Figure 3). The approach of the

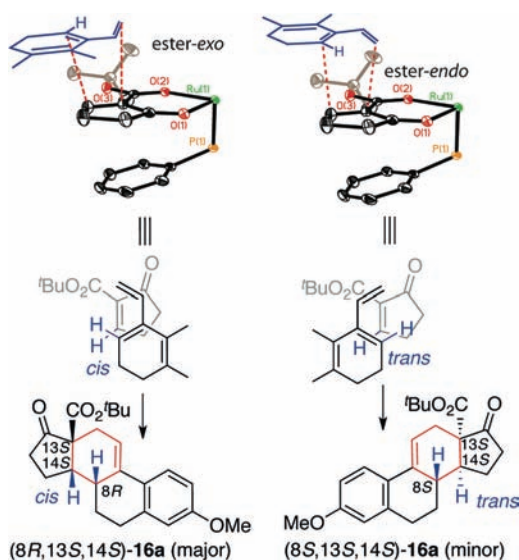


Figure 3. Sketches of the possible approaches of Dane's diene (**15**) to **7a**. Part of the methoxybenzene ring of **15** is omitted for clarity.

diene over the ester moiety of **6a**, which would result in the formation of the ester-*endo* product, is disfavored by the bulky *tert*-butyl group. Accordingly, the reaction of **15** with the methyl ester derivative **6b** gives lower *endo*/*exo* selectivity.³⁶

Together with Yamauchi's magnesium Ph-Box system,⁴ complexes of type **7** are the only highly enantioselective catalysts for Diels–Alder reactions of alkylidene β -ketoesters, which give low enantioselectivity with typical two-point binding catalysts such as titanium(IV) TADDOLato^{4b} (TADDOL is

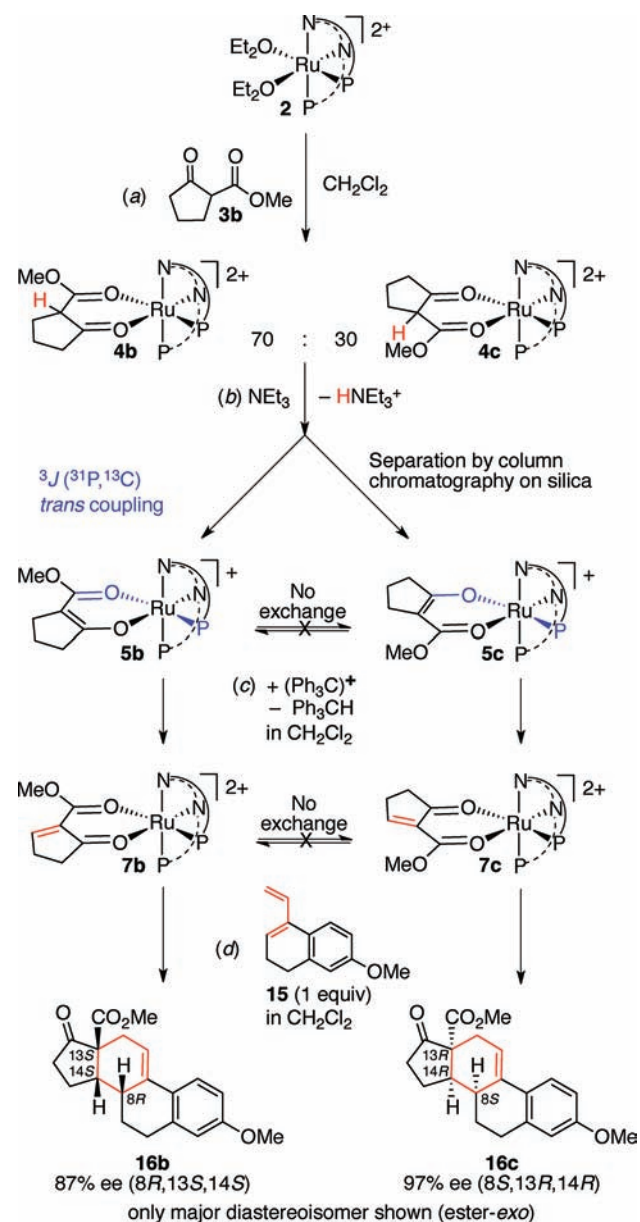
tetraaryl-1,3-dioxolane-4,5-dimethanol) and copper bisoxazoline complexes.³⁷ Therefore, the ruthenium PNNP catalysts extend the scope of Diels–Alder reactions in the challenging task of enantioselective formation of all-carbon quaternary centers, which is an area of intense research.³⁸ Also, as Corey has recently reported a procedure to convert the 18-C-methyl analogue of **16** (that is, with Me instead of CO₂R, Scheme 2b) to estrone methyl ether,^{39a,b} the reaction with Dane's diene is potentially useful in the synthesis of enantiomerically pure estrone derivatives functionalized at the α -carbonyl bridgehead position. Such biomolecules are interesting in view of their possible application in the treatment of hormone-dependent breast cancer as an inhibitor of steroidogenic enzymes^{39c–e} or as an antimicrotubule agent.^{39f} The possibility to obtain both *ent*- and *nat*-estrone derivatives is appealing, because the two enantiomeric forms of steroids usually show fundamentally different behavior.^{39g}

Catalytic Ficini Reaction. In its original version, the Ficini reaction is the [2 + 2] cycloaddition of an ynamine onto an enone⁴⁰ and has been extended to the less reactive ynamides⁴¹ only recently. In particular, sulfonyl-substituted ynamides have been shown to react with cyclohexenone in the presence of a high loading of a CuCl₂/AgSbF₆ catalyst, but no diastereoselectivity was observed with chiral ynamides.⁴² Therefore, we were pleased to discover that [Ru(OEt₂)₂(PNNP)](PF₂)₆ (**2**) (10 mol %) catalyzes the enantioselective [2 + 2] cycloaddition between unsaturated β -ketoesters **6a** (R¹ = ^tBu) or **6c** (R¹ = Et) and *N*-benzyl-*N*-(cyclohexylethynyl)-4-methylbenzenesulfonamide (**17**). The corresponding amidocyclobutenes **18** are formed with moderate to good enantioselectivity as the first example of an enantioselective Ficini reaction (Scheme 3). Further examples of cyclobutenamides of type **18**, which belong to a new class of products that feature enantioselective formation of an all-carbon stereocenter at the bridgehead position of a highly strained unsaturated [3.2.0] bicycle, have been described in a preliminary report and their structure and absolute configuration have been ascertained.¹⁶

Unlike the Diels–Alder reactions, which require an excess of the diene, nearly stoichiometric amounts of the ynamide (1.1 equiv of **17**) gave high yields. The reaction tolerates different substituents on the ynamide, but an electron-donating alkyl substituent (benzyl or methyl) must be combined with an electron-withdrawing sulfonyl group (tosyl, mesyl, or 4-methoxyphenylsulfonyl). The resulting balance of electronic effects had to be optimized to give sufficient reactivity in the catalytic reaction without promoting the background reaction. Phenyl, *n*-hexyl, cyclohexyl, and other groups are tolerated in the β -position to the nitrogen moiety. At difference with the Diels–Alder reactions, which are run at room temperature and mostly in a 1:1 CH₂Cl₂/Et₂O mixture, the optimized conditions for the Ficini reaction require heating at 55 °C in a sealed tube over 24 h in pure CH₂Cl₂.

The enantioselectivity is higher with the *tert*-butyl derivative **6a** than with the smaller 2-ethoxycarbonyl-2-cyclopenten-1-one (**6c**) (Scheme 3). This trend has already been observed in the Diels–Alder reaction, in which the *tert*-butyl derivative **6a** performs better than the methyl analogue **6b** (Table 2, entries 4, 9, and Scheme 2b), and in the previously reported transformations of the saturated β -ketoesters **3**.^{12a,14} As the coordination of **6a** to the Ru/PNNP fragment gives the adduct **7a** as a single diastereoisomer, we speculated that the lower enantioselectivity observed with the less bulky methyl and ethyl

Scheme 4. Synthesis of 7b/7c and Stoichiometric Diels–Alder Reaction with Dane’s Diene



esters may result from imperfect diastereoselectivity of the binding of the unsaturated β -ketoester to ruthenium. Some experiments designed to explain these observations are described below and summarized in Scheme 4.

Stereoselectivity of β -Ketoester Binding. $[\text{Ru}(\text{OEt}_2)_2(\text{PNNP})](\text{PF}_6)_2$ (2) was treated with the alkylidene β -ketoesters **6a–c** (1.2 equiv) in CD_2Cl_2 , and the solutions were analyzed by ^{31}P NMR spectroscopy after a reaction time of 15 min. A single product (featuring an AX pattern at δ 63.2/50.4) was observed in case of the bulky ester **6a**, whereas two main species were observed for the analogous reactions with the methyl ester **6b** (δ 64.3/50.5 and δ 62.6/49.8, 7:1 ratio) and ethyl ester **6c** (δ 63.1/49.6 and δ 61.5/48.6, 5:1 ratio). We assign the two additional signals observed for **6b** and **6c** to different diastereoisomers of $[\text{Ru}(\text{6})-(\text{PNNP})]^{2+}$ (7), which was independently proven in the case of the methyl derivative **6b**.

To that end, $[\text{Ru}(\text{OEt}_2)_2(\text{PNNP})]^{2+}$ (2) was treated with 2-methoxycarbonylcyclopentanone (**3b**) (1.1 equiv) in CD_2Cl_2 , which gave the dicationic complex $[\text{Ru}(\text{3b})(\text{PNNP})]^{2+}$ as a 70:30 mixture of diastereoisomers (**4b** and **4c**) (Scheme 4). Deprotonation with triethylamine (1.2 equiv) yielded the diastereomeric enolato complexes **5b** and **5c** in the same diastereomeric ratio, as indicated by the ^{31}P NMR spectrum (two AX patterns at δ 50.5/64.3 and δ 49.8/62.5 for **5b** and **5c**, respectively). Separation by column chromatography on silica gave pure **5b** and **5c**, which show different physical and chemical properties. The major isomer **5b** is a red crystalline solid and is significantly more soluble in CH_2Cl_2 and CHCl_3 than **5c**, which is an orange powder.

The ^{13}C NMR shifts of the enolized keto and ester moieties (**5b**: δ 193.4, 167.5; **5c**: δ 191.2, 168.0) are very similar to those of the *tert*-butyl ester analogue **5a** (δ 192.0, 168.3).^{12a,b} In the major diastereoisomer **5b**, the ester ^{13}C NMR signal at δ 167.5 (but not that of the enolized keto moiety at δ 193.4) shows coupling to phosphorus ($^3J_{\text{P,C}} = 1.5$ Hz), which is diagnostic of a *trans* arrangement of the ester and phosphine groups. Thus, **5b** has the same structure as the *tert*-butyl analogue **5a**, in which the ester group of the metal-bound β -ketoester is *trans* to P(2) (as indicated by the $^3J_{\text{P,C}}$ of 1.5 Hz to CO_2Bu). In the minor diastereoisomer **5c**, the signal of the ester moiety at δ 168.0 shows no P,C-coupling, whereas a $^3J_{\text{P,C}}$ of 1.6 Hz is observed for the signal of the enolized keto moiety at δ 191.2, which is thus *trans* to the phosphine (Scheme 4).

The diastereomeric enolato complexes **5b** and **5c** have similar ^1H NMR spectra, except for the ester methyl signal, which is distinctively shifted to lower frequency in the minor isomer **5c** (δ 2.63) as compared to **5b** (δ 3.20), probably because of the ring current of the aromatic framework of the PNNP ligand (as suggested by the X-ray structure of **5c**, see below). Complexes **5b** and **5c** can be stored at room temperature under protective gas atmosphere in the solid state for months without signs of decomposition or interconversion. Also, no isomerization is observed in CD_2Cl_2 solution over 24 h, even in the presence of diethyl ether as a coordinating cosolvent in 1:1 ratio to CD_2Cl_2 .

X-ray Structures of (*rac*)-5b** and (*rac*)-**5c**.** The enolato complex $(\text{rac})\text{-}[\text{Ru}(\text{3b-H})(\text{PNNP})]\text{PF}_6$ was prepared from the racemic (*R,R*),(*S,S*)-PNNP ligand as mixture of a major (**5b**) and minor (**5c**) diastereoisomer, which were separated by column chromatography and crystallized by layering *n*-pentane over CH_2Cl_2 and dilute CHCl_3 solutions, respectively. Both (*rac*)-**5b** and (*rac*)-**5c** contain a discrete complex cation and the hexafluorophosphate anion in the asymmetric unit, as well as disordered solvent molecules. For both diastereoisomers **5b** and **5c**, the enantiomer containing the (*S,S*)-PNNP ligand (as used in catalysis) is depicted in Figure 4.

In the major diastereoisomer **5b**, the coordination sphere of ruthenium is a distorted octahedron with the OC-6-42-*A* absolute configuration³² at ruthenium, and the (*S,S*)-PNNP ligand is in the Λ -*cis*- β configuration as in **7a** (Figure 1). As observed in solution by NMR spectroscopy, the enolato ligand binds with the keto oxygen O(1) *trans* to N(1) and with the ester carbonyl oxygen O(2) *trans* to P(2), as in the *tert*-butyl analogues **5a** and **7a**. The minor diastereoisomer **5c** exhibits the same *cis*- β configuration of the (*S,S*)-PNNP ligand, but the enolized β -ketoester binds with the ester group *trans* to N(1) and exposes the opposite enantioface (*re* in **5b** vs *si* in **5c**). Thus, the absolute configuration is OC-6-43-*A*.³² For convenience, selected interatomic distances of **5b** and **5c** are

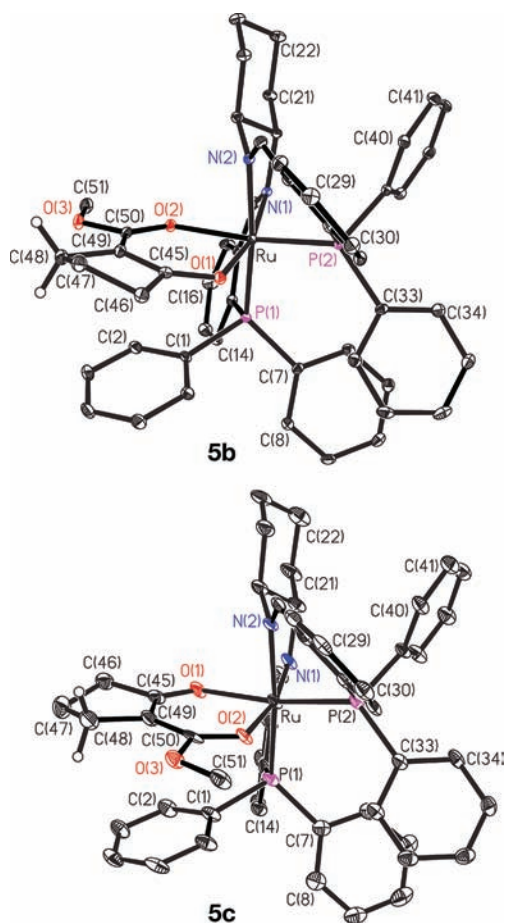


Figure 4. ORTEP drawings of (OC-6-42-A-(*S,S*))-**5b** (major diastereoisomer) and (OC-6-43-A-(*S,S*))-**5c** (minor diastereoisomer) (ellipsoids at 30% probability).

compared with those of the *tert*-butyl analogue **5a** and of the unsaturated analogue **7a** in Table 1 and Chart 3.

Overall, the metrical parameters of **5b** and **5c** (see Supporting Information) show that the conformation of the PNNP ligand are very similar in both diastereoisomers, which suggests that there is no strong steric preference for the major diastereoisomer **5b**. In contrast, the patterns observed for the Ru–O distances largely differ in the two diastereoisomers. In **5b**, the keto oxygen O(1), which bears the larger negative partial charge and is trans to nitrogen, features a much shorter Ru–O bond than the ester carbonyl, which is trans to phosphorus (2.086(2) vs 2.128(2) Å). Thus, in **5b**, the stronger oxygen donor is trans to the ligand with the lower trans influence (imine) as compared to phosphine, which is the electronically favored situation. In the minor isomer **5c**, Ru–O(1) and Ru–O(2) are identical within experimental error, indicating that the effects of enolization and of trans influence cancel out. As the stronger donor (the keto group) is trans to phosphine, this configuration is slightly electronically disfavored. Space-filling models show that the small methyl ester group can easily be accommodated both in **5b** and **5c** (Figure 5), which suggests that the weak diastereoselectivity (70:30) observed for the methyl ester mainly results from electronic factors. As these are similar in the methyl derivatives **5b/5c** and in the *tert*-butyl analogue **5a**, the formation of a single diastereoisomer in the case of the bulky *tert*-butyl ester complex **5a** is mainly dictated by steric factors.

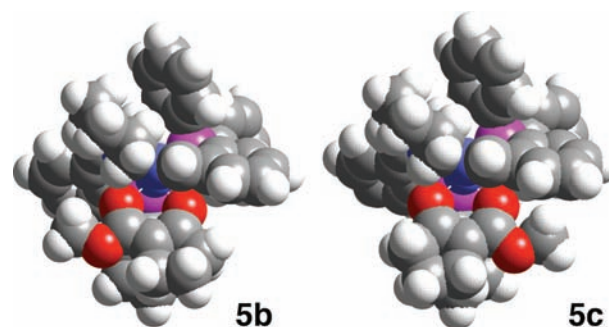
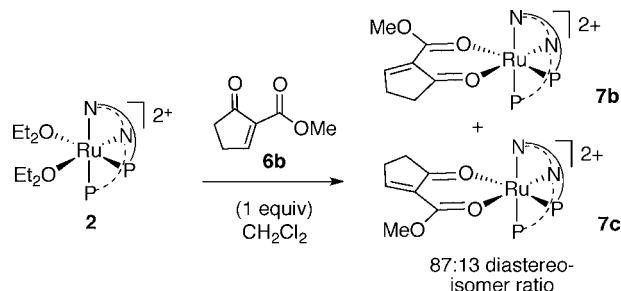


Figure 5. Space-filling representations (Cerius²) of the X-ray structures of (OC-6-42-A-(*S,S*))-**5b** (major diastereoisomer) and (OC-6-43-A-(*S,S*))-**5c** (minor).

Synthesis of 7b and 7c. The diastereomerically pure enolato complex **5b** (or **5c**) reacts instantaneously with (Ph₃C)PF₆ (1.05 equiv) in CD₂Cl₂ to give the substrate/catalyst adduct **7b** (or **7c**) (Scheme 4c), as indicated by the color change of the reaction solution from red-orange to yellow. When pure major isomer **5b** was used, **7b** was the only product, whereas pure **5c** formed **7c** only. Hence, the reaction is stereospecific. When the hydride abstraction was performed with the 70:30 diastereoisomeric mixture of **5b** and **5c** (that is, without previous chromatographic separation), **7b** and **7c** were formed in the same ratio of the starting materials. In contrast, the addition of the alkylidene β -ketoester **6b** to [Ru(OEt₂)₂(PNNP)]²⁺ (**2**) gave **7b/7c** with a diastereomeric ratio of 87:13 (Scheme 5).

Scheme 5. Direct Synthesis of 7b/7c from 2 and 6b



Like **7a**,⁴³ the highly reactive and catalytically active complexes **7b** and **7c** cannot be isolated and were characterized in solution by ¹H, ³¹P, and ¹³C NMR spectroscopy by analogy to **7a**. As in the case of **5c**, the minor diastereoisomer of the alkylidene β -ketoester complex, **7c**, exhibits a distinctive low-frequency shift of the methyl ester signal (**7b**: δ 3.62, **7c**: δ 2.94). The diagnostic coupling (³J_{P,C}) to the trans carbonyl group (see **5b** and **5c** above) is not resolved in **7c** but is observed in **7b** (³J_{P,C} = 1.5 Hz). After 12 h in CD₂Cl₂, the pure diastereoisomers **7b** and **7c** undergo partial decomposition to unidentified products, but there is no conversion to the other diastereoisomer, which confirms that they do not equilibrate under these conditions (Scheme 4). The complexes are configurationally stable also in the presence of a coordinating cosolvent such as diethyl ether (1:1 with CD₂Cl₂), which fails to promote ligand exchange.

Stoichiometric Diels–Alder Reactions with 7a–c. The alkylidene β -ketoester complexes **7a–c**, formed in situ from the corresponding saturated β -ketoesters **3a–c** as described above, were used in a series of stoichiometric reactions with Dane’s

diene (**15**) to model a single catalytic cycle (Table 3). The substrate/catalyst adducts **7b** and **7c** with the methyl ester

Table 3. Diels–Alder Reactions with Dane’s Diene (15**) and **2** or **7^a****

entry	complex	mol %	added substrate	ee (%)
1	7a	100	–	90
2	7b	100	–	87
3	7c	100	–	97 ^b
4	7b/7c (87:13) ^c	100	–	56
5	7b/7c (70:30) ^d	100	–	34
6	7a	10	6a	86
7	2	10	6a	85
8	7b	10	6b	72
9	7b^e	5	6b	79
10	7b/7c (87:13) ^c	10	6b	51
11	7c^e	5	6b	60

^aSee Supporting Information for details. Absolute configuration of the product is 8*R*,13*S*,14*S*, unless otherwise stated. ^bAbsolute configuration is 8*S*,13*R*,14*R*. ^cPrepared from **2** and **6b**; see text and Scheme 5. ^dPrepared from **2** and **3b** (see ref 46). ^eReaction time was 48 h.

substrate **6b** were prepared either as pure diastereoisomers or as a mixture with predetermined diastereoisomeric ratio. The diastereomerically pure complex **7a**, which contains (*S,S*)-PNNP and *tert*-butoxycarbonyl-2-cyclopenten-1-one (**6a**), reacted with **15** (1.1 equiv) to give the Diels–Alder adduct **16a** in 87% yield and with 90% ee, as indicated by chiral HPLC analysis after workup (Table 3, entry 1). The absolute configuration of **16a** is 8*R*,13*S*,14*S*, in agreement with an attack from the upper face of the substrate (Figure 3). Accordingly, the major diastereoisomer of the methyl ester derivative **7b** forms the same enantiomer of **16b** with 87% ee (entry 2), whereas the minor diastereoisomer **7c** reacts with the opposite sense of induction to give (8*S*,13*R*,14*R*)-**16b** with 97% ee (entry 3). As discussed for **7a**, the preferred approach of the diene is over the cyclopentenone ring in both cases (ester-*exo*, Figure 3). However, the diastereoselectivity drops from 26:1 for **7a** to approximately 5:1 for **7b** and **7c** with the same trend observed in catalysis (Scheme 2b).

The fact that the **7c** gives enantioselectivity higher than that of the major diastereoisomer **7b** can be explained on the basis of the X-ray structures of the related enolato complexes **5b** and **5c**, which can act as models for the substrate adducts **7b** and **7c** (Figure 6).⁴⁴ The C(49)⋯Ru–P(1)–C(1) torsion angle (–4.9(3)° vs –11.4(1)°) and the C(1)⋯C(49) and C(4)⋯C(48) separations are much smaller in **5c** than in **5b**. Thus, the C(1)–C(6) phenyl ring is closer and better aligned with the enolato moiety in the minor diastereoisomer **5c**, which enhances the shielding of the re face of the alkylidene β -ketoester and explains the higher enantioselectivity of the stoichiometric reaction of Dane’s diene **15** with **7c** than with **7b**.⁴⁵

To double-check these results, the stoichiometric reactions with Dane’s diene **15** were run with diastereoisomeric mixtures of **7b** and **7c** in different ratios. A 87:13 diastereoisomeric mixture of **7b** and **7c**, prepared under the same conditions of catalysis (that is, by addition of **6b** (1 equiv) to a solution of **2**, Scheme 5), was treated with Dane’s diene **15**. The resulting Diels–Alder adduct **16b** was formed with 56% ee, which is close to the enantioselectivity of 51% ee observed under catalytic conditions (Table 3, entries 4 and 10). At difference, a 70:30

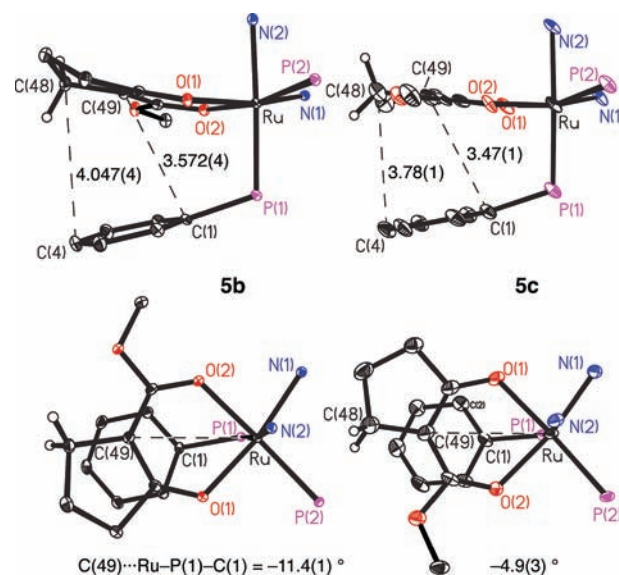


Figure 6. Partial ORTEP views of **5a** and **7a** (the PNNP framework is omitted for clarity, except for the C(1)–C(6) phenyl ring). The angles between the C(1)–C(6) phenyl ring and the C(45)–C(49)–C(50) plane are 26.6(2) and 18.0(7)°, respectively.

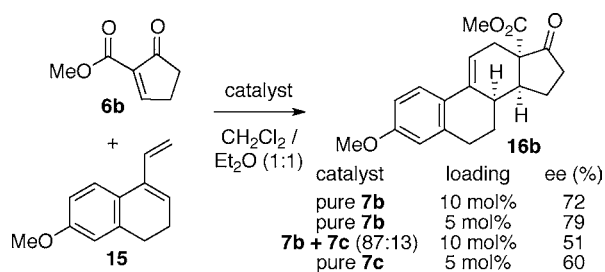
diastereoisomeric mixture of **7b** and **7c** (Scheme 4)⁴⁶ gave the estrone derivative **16b** with 34% ee (entry 5). Taking into account the diastereomeric ratio (70:30) and the inherent enantioselectivity of the cycloaddition reaction between the pure diastereoisomers **7b** and **7c** and **15** as determined from the above stoichiometric reactions (87% ee for **7b**, 97% ee for **7c**), we calculate a theoretical value of 36% ee, which is in good agreement with the experimental value of 34% ee. These results confirm that the enantioselectivity of the Diels–Alder reaction is controlled by the diastereoselectivity of the coordination of the unsaturated β -ketoester to ruthenium.

Effect of Catalyst Stereochemistry. The substrate/catalyst adduct **7a** with *tert*-butyl ester **6a** catalyzes the Diels–Alder reaction between Dane’s diene (**15**) with essentially the same enantioselectivity as the Et₂O adduct **2** (both 10 mol %) (86 and 85% ee, Table 3, entries 6, 7). These values are only slightly lower than in the corresponding stoichiometric reaction (90% ee, entry 1) and are in agreement with the observation that the substrate/catalyst adduct **7a** is formed as a single diastereoisomer both by hydride abstraction from **5a** and by reaction of **2** with β -ketoester **6a**.

Then, to study the effect of the diastereomeric composition of the catalyst on the stereochemical course, the Diels–Alder reaction of **15** was performed with substrate/catalyst adducts of the methyl derivative **6b** with different diastereoisomeric compositions (Scheme 6). The pure diastereoisomer **7b** as catalyst gave **16b** with an enantioselectivity significantly higher than that of **2**, which reacts with **6b** to give a 87:13 diastereoisomeric mixture of **7b** and **7c** (72 vs 51% ee, Table 3, entries 8–10). The increase is too large to be caused by the high enantioselectivity obtained in the first catalytic cycle (which must be close to 87% ee, as indicated by the stoichiometric reaction, entry 2) and may suggest a memory effect in which the substitution of the product by the substrate occurs with retention of configuration at the metal.

However, monitoring the reaction between **6b** and **15** with diastereomerically pure **7b** as catalyst (5 mol %) shows that the

Scheme 6. Catalytic Reactions with Preformed Substrate/Catalyst Adducts 7b/7c



enantioselectivity gradually drops over 72 h (Table 4). This is in agreement with the evolution of the catalyst from the initially

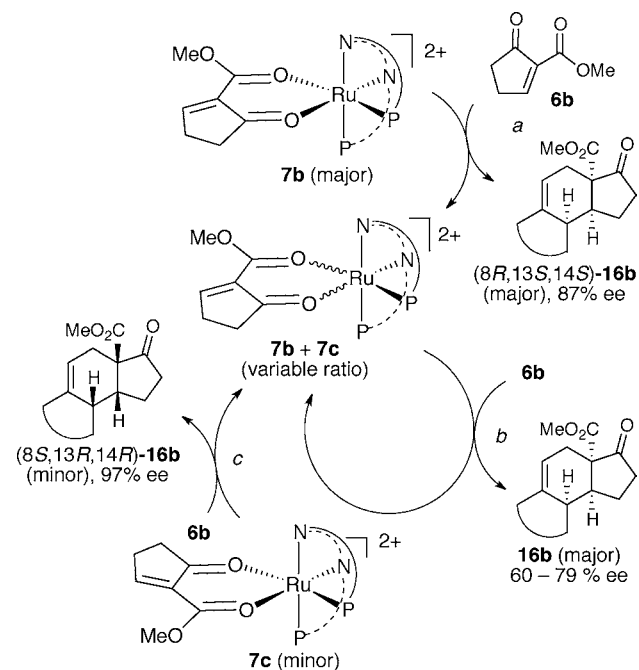
Table 4. Enantioselectivity Change during the Reaction of 6b with 15 Catalyzed by 7b.^a

entry	time (h)	ee (%)
1	0.5	83
2	1	80
3	6	79
4	24	76 ^b

^aIn a standard catalytic run with 7b (5 mol %), samples (0.1 mL) were taken with a syringe, filtered through a pad of silica, and analyzed by chiral HPLC. ^bNo changes after 72 h.

present diastereomerically pure 7b (which forms 16b with 87% ee) to a mixture of 7b and of the minor diastereoisomer 7c upon coordination of a new substrate molecule (Scheme 7a,b).

Scheme 7. General Stereochemical Course of the Catalytic Diels–Alder Reaction with 6b and 15



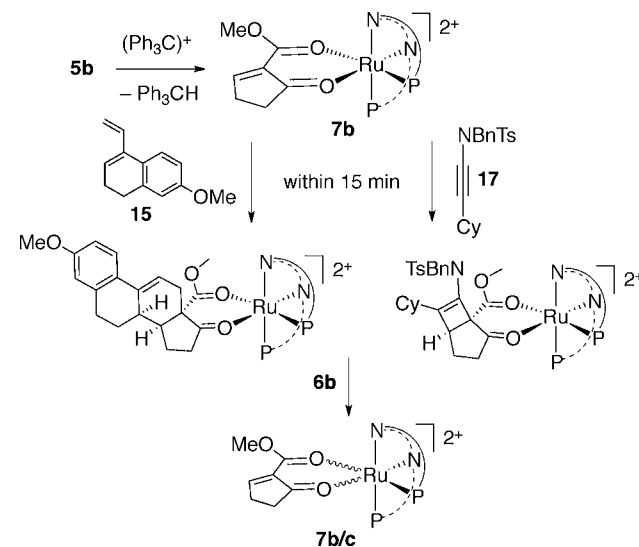
The formation of 7c, which gives the opposite enantiomer of 16b, accounts for the decreasing enantioselectivity. Pure 7c as catalyst *ceteris paribus* gave the same sense of induction as that for 2 and the major diastereoisomer 7b, which rules out a memory effect. Because of the inverse sense of induction at the

onset of the catalytic reaction, the enantioselectivity was lower with 7c than with 7b (60 vs 79% ee, Table 3, entries 11 and 9) but surprisingly higher than with catalyst 2 (51% ee, entry 10).⁴⁷

Diels–Alder Product Displacement from Catalyst.

After the stoichiometric reaction of the substrate/catalyst adducts with Dane's diene (15), the next series of experiments was designed to study the displacement of the product (16) from the catalyst by a substrate molecule, which closes the catalytic cycle. To simulate a single turnover of the catalytic cycle, diastereomerically pure 7b was treated with diene 15 (1 equiv) in CD₂Cl₂ in an NMR tube. The ³¹P NMR spectra of the reaction solution showed that 7b had reacted quantitatively within 15 min. Apart from trace impurities, the only signals observed after this time were an AX pattern that we assign to [Ru(16b)(PNNP)]²⁺ on the basis of comparison with an authentic sample prepared from 2 and isolated 16b (Scheme 8).⁴⁸

Scheme 8. Regeneration of the Substrate/Catalyst Adduct



Then, β -ketoester 6b (1 equiv) was added to the above solution of [Ru(16b)(PNNP)]²⁺, and the regeneration of the active species 7b/c was monitored by ³¹P NMR spectroscopy (Table 5, entry 1). After 30 min, the product adduct

Table 5. Product Displacement by Substrates 6b (or 6a)^a

entry	reagent	substrate (equiv)	solvent	T (°C)	regeneration of 7b+7c (%) ^b
1	15	6b (1)	CD ₂ Cl ₂	25	35
2	15	6b (9)	CD ₂ Cl ₂	25	40
3	15	6b (1)	CD ₂ Cl ₂ / Et ₂ O ^c	25	70
4 ^d	15	6a (1)	CD ₂ Cl ₂	25	60
5	17	6b (1)	CD ₂ Cl ₂	25	5–10
6	17	6b (1)	CD ₂ Cl ₂ / Et ₂ O ^c	25	20
7	17	6b (1)	CD ₂ Cl ₂	55	100

^aAfter 30 min of reaction time between the product/catalyst adduct and 6a/b. ^bFrom the total intensity of both diastereoisomers. ^cIn a 1:1 ratio. ^dThe initial reaction of 15 with 7a took 30 instead of 15 min as with 7b/c.

[Ru(16b)(PNNP)]²⁺ was still the main species present in solution (ca. 65%). The formation of the diastereoisomeric

substrate adducts **7b** and **7c** was quantitative only after 3 h. The rate of the product/substrate exchange is unaffected by an excess of substrate **6b** (9 equiv, entry 2) but significantly accelerated in CD₂Cl₂/Et₂O (1:1) solution (entry 3). The analogous reaction between **15** and the sterically more demanding *tert*-butyl β -ketoester complex **7a** is slower than with the methyl analogue **7b**, but the dissociation of the corresponding product is faster (entry 4),⁴⁹ which possibly explains why **6a** and **6b** give a similar reaction profile in the catalytic reaction.

The above results show that (i) the equilibrium between [Ru(**16b**)(PNNP)]²⁺ and [Ru(**6b**)(PNNP)]²⁺ lies completely on the side of substrate coordination, (ii) the product/substrate exchange is slower than the cycloaddition reaction, and (iii) the resulting inhibition is operative already at the onset of the catalytic reaction (when most of the substrate is still present). We conclude that, in the reaction between **6b** and diene **15**, product release from the catalyst is slow as compared to the cycloaddition reaction, which makes it a prime candidate for the rate-determining step of the catalytic cycle. This effect is kinetic in nature, as the substrate/product ratio does not significantly affect the rate of the exchange reaction.⁵⁰ Finally, Et₂O as cosolvent accelerates the regeneration of the substrate/catalyst adduct, possibly because it assists product displacement (Table 5, entry 3). This explains why a 1:1 mixture of CD₂Cl₂ and Et₂O (1:1) gives the best results in catalysis with electron-rich, highly reactive dienes **10**, **11**, and **15** (Table 2).^{15,51}

Stoichiometric Ficini Reaction. For the sake of comparison, **7b** was treated with *N*-benzyl-*N*-(cyclohexylethynyl)-4-methylbenzenesulfonamide (**17**) under the same conditions. Complex **7b** reacted quantitatively within 15 min to give ruthenium-bound methyl-7-[*N*-benzyl-4-methylphenylsulfonamido]-6-cyclohexyl-2-oxobicyclo[3.2.0]hept-6-ene-1-carboxylate (**18**) (by comparison with an authentic sample). Upon addition of **6b**, the product/substrate exchange gave only about 5–10% of **7b/7c** after 30 min (Table 5, entry 5). A CD₂Cl₂/Et₂O (1:1) solvent mixture accelerates the displacement of the Ficini product **18** (entry 6), as observed in the Diels–Alder reaction with **15** (entry 3). However, the effect of Et₂O is not large enough to even reach the rate observed in the Diels–Alder reaction in pure CD₂Cl₂ (entry 1).

Then, the experiment was repeated in pure CH₂Cl₂ by heating at 55 °C in a sealed tube for 30 min. After cooling the sample to room temperature, the ³¹P NMR spectrum recorded immediately thereafter showed quantitative formation of **7b/c** (entry 7). This experiment also shows that the coordination equilibrium lies completely on the side of [Ru(**6b**)PNNP]²⁺, as in the case of the Diels–Alder reaction. Once again, the conditions that overcome the kinetic inhibition in the stoichiometric reaction correspond closely to those of the optimized catalytic reaction described above.¹⁶ In the next section, we discuss the origin of the slow release of the cycloaddition product from the catalyst.

Chances and Challenges of Low-Spin d⁶ Lewis Acids.

Lewis acidic catalysts are mostly based on hard, but labile, Lewis acids, such as early transition metals, lanthanides, Cu(II), and boron.^{1b} To understand the mechanism of stereoselection and rationally modify the catalyst, structural information concerning the substrate/catalyst adduct is required. However, the characterization of the catalytically active species is not a trivial task with these systems because of fast exchange reactions in solution and/or the possibility that many different complexes coexist in equilibrium. For instance, enal complexation to boron-based Lewis acids is rapidly reversible on the

NMR time scale,^{52a} and the selectivity depends only on the energy difference between the two diastereoisomeric transition states.^{52b} Such problems are often intractable, and their solution must be sought by calculation. A further example is the highly enantioselective Diels–Alder reaction of 3-cinnamoyloxazolidin-2-one and cyclopentadiene catalyzed by [TiCl₂(TADDOL)] system,⁵³ whose substrate/catalyst adduct has been the subject of debate as for its structure, configuration,⁵⁴ and even nuclearity.⁵⁵ Such uncertainties led Evans to state that “our understanding pertaining to substrate/catalyst interactions [in Diels–Alder reactions] is still in its infancy”.⁵⁶

A commonly used option to model the catalytically active species with very reactive systems is to use structurally characterized complexes with strongly coordinating, but inactive, ancillary ligands as models for the substrate/catalyst adduct. Examples of this strategy have been reported with many transition metals such as Cu(II),¹⁷ Ni(II),⁵⁷ Zn(II),⁵⁸ Rh(III),⁵⁹ and Fe(II).⁶⁰ This method, albeit useful, is intrinsically less reliable than X-ray structure determination of the substrate/catalyst adducts, as illustrated by Evans’s enantioselective Michael addition to alkylidene malonates.^{17b,61}

Therefore, a desirable requirement of a Lewis acidic catalyst is to form adducts with the substrate according to a well-defined stoichiometry that can be structurally characterized. A perusal of the literature shows that this dual requirement is met by a number of ruthenium(II) Diels–Alder catalysts such as chiral Ru(II) half-sandwich complexes, whose adducts with methyl vinyl ketone⁶² and methacrolein⁶³ have been characterized. Together with the already mentioned Ir(III) catalysts for the Nazarov cyclization,¹⁸ these are low-spin d⁶ octahedral complexes of 4d and 5d metals with middle- to strong-field ligands and hence among the most stable⁶⁴ and inert⁶⁵ coordination compounds. The low-spin d⁶ configuration is the key feature to allow for isolation of reactive intermediate and reduced rate of exchange in solution, which makes them amenable to spectroscopic investigation by NMR spectroscopy. At the same time, the inertness of the complexes is also the main disadvantage of this approach, as product release from the catalyst can be a significant issue (see above).

A further point is that d⁶ octahedral complexes typically lack the most conspicuous property of a Lewis acidic catalyst, that is, the affinity for oxygen-donor ligands. Therefore, special features must be introduced in these catalysts, such as a high positive charge (or high formal oxidation state), hard ancillary ligands, and/or strong π -acceptors.⁶⁶ Accordingly, ruthenium half-sandwich Diels–Alder catalysts either contain a strongly π -accepting bis(perfluorophenyl)diphosphinite ligand⁶² or bear a double positive charge,⁶³ whereas Eisenberg’s iridium(III) complex is dicationic and contains CO as ancillary ligand.¹⁸ In the case of [Ru(**6a**)(PNNP)]²⁺ (**7a**), the important features are the hard nitrogen donors and the dicationic nature of the complex. As for the latter issue, we have recently reported that the monocationic adducts [RuCl(OR₂)(PNNP)]⁺ (R = H or Et) are labile and exist in CD₂Cl₂ solution in equilibrium with the five-coordinate complex [RuCl(PNNP)]⁺.^{66b} Therefore, we attribute the inert nature of **7a** to a combination of several factors and in particular the chelate effect of the bidentate β -ketoester, the double positive charge, and the low-spin d⁶ configuration of these octahedral complexes.⁶⁷

Finally, the absence of a background reaction with poorly reactive dienophiles, as observed in the case of the reaction of alkylidene β -ketoesters with dienes and ynamides, is considered

to be an unfavorable basis for highly enantioselective catalytic Diels–Alder reactions.³ Therefore, we speculate that the dicationic nature of catalyst **7** and the combination of hard (N) and soft (P) donors successfully contribute to give a highly oxophilic, though mild, Lewis acid that is able of activating alkylidene β -ketoesters without triggering undesired side-reactions such as polymerization. The above studies show that the ruthenium PNNP-catalyzed reactions are on a narrow path between low reactivity of the alkylidene β -ketoester toward the diene and slow product release, which possibly provides another explanation why these reactions have challenged synthetic organic chemists for so long.

CONCLUSION AND OUTLOOK

Hydride abstraction from enolato Ru/PNNP complexes gives well-defined, easily characterized dicationic complexes containing alkylidene β -ketoesters that are efficient asymmetric catalysts for Diels–Alder and Ficini reactions with dienes and ynamides, respectively. The resulting products are highly functionalized bicyclic molecules containing all-carbon stereocenters. The ruthenium/PNNP complexes reported herein are noticeable because they expand the scope of cycloaddition reactions to unsaturated β -ketoesters, which are rarely used in these reactions, and are a rare example of fully characterized substrate/catalyst adducts. The structure and stoichiometric reactions of such adducts are easily studied and yield valuable information on the stereochemical course of the reaction and on the relative rate of the cycloaddition and product release steps. These insights explain the steric and solvent effects observed in catalysis. In perspective, the Ru/PNNP catalyst may allow for a fast screening and optimization of the catalytic system with different substrates and reagents. This includes the tuning of the PNNP ligand with electron-withdrawing or -donating substituents to optimize the Lewis acidity of the system. In fact, PNNP ligands are easily modified⁶⁸ and form a family of ligands that may find broad application in organic synthesis.

ASSOCIATED CONTENT

Supporting Information

General experimental protocols, characterization data for new compounds, and crystallographic data (CIF). This material is available free of charge via the Internet at <http://pubs.acs.org>.

AUTHOR INFORMATION

Corresponding Author

Mezzetti@inorg.chem.ethz.ch

ACKNOWLEDGMENTS

We thank Dr. Pietro Butti (ETH Zürich) for the X-ray structure of **7a**.

REFERENCES

(1) Reviews of Diels–Alder reactions: (a) Corey, E. J. *Angew. Chem., Int. Ed.* **2002**, *41*, 1650. (b) Evans, D. A.; Johnson, J. S. In *Comprehensive Asymmetric Catalysis*; Jacobsen, E. N.; Pfaltz, A.; Yamamoto, H., Eds., Springer: Heidelberg, 1999; Vol. 3, pp 1178–1235. (c) Carruthers, W. *Cycloaddition Reactions in Organic Synthesis*; Pergamon: Oxford, 1990. (d) Kobayashi, S.; Jørgensen, K. A. *Cycloaddition Reactions in Organic Synthesis*; Wiley: Weinheim, 2001. (e) Da, H.; Ding, H. In *Handbook of Cyclization Reactions*; Ma, S., Ed.; Wiley: Weinheim, 2009; Vol. 1, pp 1–57.

(2) Evans, D. A.; Johnson, J. S. In *Comprehensive Asymmetric Catalysis*; Jacobsen, E. N.; Pfaltz, A.; Yamamoto, H., Eds.; Springer: Heidelberg, 1999; Vol. 3, p 1229–1230.

(3) Ryu, D. H.; Lee, T. W.; Corey, E. J. *J. Am. Chem. Soc.* **2002**, *124*, 9992.

(4) (a) Honda, Y.; Date, T.; Hiramatsu, H.; Yamauchi, M. *Chem. Commun.* **1997**, 1411. (b) Yamauchi, M.; Aoki, T.; Li, M. Z.; Honda, Y. *Tetrahedron: Asymmetry* **2001**, *12*, 3113.

(5) Marx, J. N.; Cox, J. H.; Norman, L. R. *J. Org. Chem.* **1972**, *37*, 4489.

(6) Liu, H. J.; Ngooi, T. K.; Browne, E. N. C. *Can. J. Chem.* **1988**, *66*, 3143.

(7) For instance, the reaction of 2-ethoxycarbonyl-2-cyclohexen-1-one with 1-methylbuta-1,3-diene has been carried out with the stoichiometric activation of the diene by a cobalt complex in the presence of a large excess (4 equiv) of the dienophile over 3 days in refluxing THF and subsequent cleavage of the cobalt complex from the Diels–Alder product, see: Richardson, B. M.; Welker, M. E. *J. Org. Chem.* **1997**, *62*, 1299.

(8) (a) Shizuka, M.; Snapper, M. *Angew. Chem., Int. Ed.* **2008**, *47*, 5049. (b) Piovesana, S.; Schirotoma, D. M. S.; Tulli, L. G.; Monaco, M. R.; Bella, M. *Chem. Commun.* **2010**, *46*, 5160. (c) Chapdelaine, D.; Belzile, J.; Deslongchamps, P. *J. Org. Chem.* **2002**, *67*, 5669. (d) Bernardi, A.; Colombo, G.; Scolastico, C. *Tetrahedron Lett.* **1996**, *37*, 8921. (e) Li, W.; Liu, X.; Zhou, X.; Lee, C.-S. *Org. Lett.* **2010**, *12*, 548.

(9) Mezzetti, A. *Dalton Trans.* **2010**, 7851.

(10) PNNP = (*S,S*)-*N,N'*-bis[*o*-(diphenylphosphino)benzylidene]cyclohexane-1,2-diamine.

(11) Gao, J. X.; Ikariya, T.; Noyori, R. *Organometallics* **1996**, *15*, 1087.

(12) (a) Santoro, F.; Althaus, M.; Bonaccorsi, C.; Gischig, S.; Mezzetti, A. *Organometallics* **2008**, *27*, 3866. (b) Althaus, M.; Bonaccorsi, C.; Mezzetti, A.; Santoro, F. *Organometallics* **2006**, *25*, 3108. (c) Bonaccorsi, C.; Althaus, M.; Becker, C.; Togni, A.; Mezzetti, A. *Pure Appl. Chem.* **2006**, *78*, 391.

(13) Toullec, P. Y.; Bonaccorsi, C.; Mezzetti, A.; Togni, A. *Proc. Natl. Acad. Sci. U.S.A.* **2004**, *101*, 5810.

(14) Althaus, M.; Becker, C.; Togni, A.; Mezzetti, A. *Organometallics* **2007**, *26*, 5902.

(15) (a) Schotes, C.; Mezzetti, A. *J. Am. Chem. Soc.* **2010**, *132*, 3652. (b) Schotes, C.; Mezzetti, A. *Chimia* **2011**, *65* (4), 231.

(16) Schotes, C.; Mezzetti, A. *Angew. Chem., Int. Ed.* **2011**, *50*, 3072.

(17) (a) Evans, D. A.; Rovis, T.; Kozłowski, M. C.; Tedrow, J. S. *J. Am. Chem. Soc.* **1999**, *121*, 1994. (b) Evans, D. A.; Rovis, T.; Kozłowski, M. C.; Downey, C. W.; Tedrow, J. S. *J. Am. Chem. Soc.* **2000**, *122*, 9134.

(18) (a) Janka, M.; He, W.; Frontier, A. J.; Flaschenriem, C.; Eisenberg, R. *Tetrahedron* **2005**, *61*, 6193. (b) Janka, M.; He, W.; Haedicke, I. E.; Fronczek, F. R.; Frontier, A. J.; Eisenberg, R. *J. Am. Chem. Soc.* **2006**, *128*, 5312.

(19) (a) Structurally characterized TiCl₄-adducts with alkylidene β -ketoesters have been used in Ziegler–Natta catalysis, which does not involve activation of the C=C double bond; see: (b) Kakkonen, H. J.; Pursiainen, J.; Pakkanen, T. A.; Ahlgrén, M.; Iiskola, E. *J. Organomet. Chem.* **1993**, *453*, 175.

(20) The slow oxidation of the Ru(II) catalyst to Ru(III) was considered as a possible cause of the observed increase of enantioselectivity with time, which we eventually explained with the accumulation of the fluorinated β -ketoester during the catalytic reaction.¹⁴

(21) (a) The shielding constant σ for the chemical shift of non-H nuclei mainly depends on the paramagnetic term σ_{para} , which is influenced by the p-electron excitation energy ΔE , and on the expectation value r_{2p} for the distance of a 2p-electron from the nucleus:^{21b}

$$\sigma_{\text{para}} = -\frac{1}{\Delta E r_{2p}^3}$$

where ΔE is the energy difference for the $\pi \rightarrow \pi^*$ transition, that is, the HOMO–LUMO gap of the coordinated enone ester **6a**,

and r_{2p} is determined mostly by the charge density at the corresponding carbon atom. We suggest that the highly deshielded carbon resonance at δ 188.3 in **7a** results from the polarization caused by the coordination to the dicationic ruthenium PNNP fragment, which lowers the energy of the enone π^* -orbital (small ΔE) and contracts the p-orbital coefficient (reduced electron density on C). (b) Wehrli, F. W.; Marchand, A. P.; Wehrli, S. *Interpretation of Carbon-13 NMR Spectra*, 2nd ed.; Wiley: Chichester, 1988; pp 34–38.

(22) Houk, K. N.; Strozler, R. W. *J. Am. Chem. Soc.* **1973**, *95*, 4094.

(23) Cheng, T.-Y.; Szalda, D. J.; Zhang, J.; Bullock, R. M. *Inorg. Chem.* **2006**, *45*, 4712.

(24) Gombert, M. *J. Am. Chem. Soc.* **1900**, *22*, 757.

(25) Jung, M. E.; Brown, R. W. *Tetrahedron Lett.* **1978**, *31*, 2771.

(26) Jung, M. E.; Pan, Y.-G. *J. Org. Chem.* **1977**, *42*, 3961.

(27) Selected examples: (a) Weng, W.; Chen, C.-H.; Foxman, B. M.; Ozerov, O. V. *Organometallics* **2007**, *26*, 3315. (b) O'Connor, E. J.; Kobayashi, M.; Floss, H. G.; Gladysz, J. A. *J. Am. Chem. Soc.* **1987**, *109*, 4837. (c) Tam, W.; Lin, G. Y.; Wong, W. K.; Kiel, W. A.; Wong, V. K.; Gladysz, J. A. *J. Am. Chem. Soc.* **1982**, *104*, 141. (d) Kiel, W. A.; Lin, G.-Y.; Gladysz, J. A. *J. Am. Chem. Soc.* **1980**, *102*, 3299.

(28) Carter, C. A. G.; Casty, G. L.; Stryker, J. M. *Synlett* **2001**, 1046.

(29) (a) Liotta, D.; Barnum, C.; Puleo, R.; Zima, G.; Bayer, C.; Kezar, H. S. *J. Org. Chem.* **1981**, *46*, 2920. (b) Baker, R.; Selwood, D. L.; Swain, C. J.; Webster, N. M. H. *J. Chem. Soc., Perkin Trans. 1* **1988**, *3*, 471.

(30) Schultz, A. G.; Holoboski, M. A. *Tetrahedron Lett.* **1993**, *34*, 3021.

(31) Chou, H.-H.; Hsieh, M.-T.; Liu, H.-J.; Ly, T. W.; Wu, H.-M.; Wu, Y.-K. *Org. Lett.* **2009**, *11*, 1673.

(32) (a) *Nomenclature of Inorganic Chemistry: IUPAC Recommendations 2005*; Connelly, N. G.; Hartshorn, R. M.; Damhus, T.; Hutton, A. T., Eds.; RSC Publishing: Cambridge, 2005; pp 174–199. (b) Sloan, T. E. In *Topics in Inorganic and Organometallic Stereochemistry*; Geoffroy, G. L., Ed.; Topics in Stereochemistry; Wiley: New York, 1981; Vol. 12, pp 1–36. (c) Von Zelevsky, A. *Stereochemistry of Coordination Compounds*; Wiley: Chichester, 1996. (d) Knof, U.; von Zelevsky, A. *Angew. Chem., Int. Ed.* **1999**, *38*, 302–322.

(33) This complex, which was obtained upon attempts to crystallize the β -ketoester complex **4a**, is probably formed by acid-catalyzed hydrolysis of **3a**; see ref 12a.

(34) Huheey, J. E.; Keiter, E. A.; Keiter, R. L. *Inorganic Chemistry: Principles of Structure and Reactivity*, 4th ed.; Harper Collins College Publishers: New York, 1993; pp A–30.

(35) Interestingly, this rearrangement does not involve the P(1) atom connected to the C(1)–C(6) phenyl ring, the C(49)–Ru–P(1) angle remaining nearly unchanged (92.52(6) vs 91.27(5)°, Table 1), as compared to the large reduction of the angle between the substrate and phenyl-ring planes (see above).

(36) (a) Electronic factors are believed to influence the diastereoselectivity of Diels–Alder reactions via secondary orbital overlaps (SOO).^{36b,c} However, the difference in SOO between the keto and the ester carbonyl group must be small in comparison to the effect of the steric difference between cyclopentenone ring and ester moiety, see ref 15b. (b) Fleming, I. *Molecular Orbitals and Organic Chemical Reactions*, Student ed., 1st ed.; John Wiley & Sons Ltd.: Chichester, 2009; pp 235–238. (c) Ohwada, T. In *Topics in Current Chemistry*, Inagaki, S., Ed.; Springer: Berlin/Heidelberg, 2009; Vol. 289, pp 161–171.

(37) Schotes, C.; Mezzetti, A. *J. Org. Chem.* **2011**, *76*, 5862.

(38) Trost, B. M.; Jiang, C. *Synthesis* **2006**, 369.

(39) (a) Yeung, Y. Y.; Chein, R. J.; Corey, E. J. *J. Am. Chem. Soc.* **2007**, *129*, 10346. (b) Canales, E.; Corey, E. J. *Org. Lett.* **2008**, *10*, 3271. (c) Vicker, N.; Lawrence, H.; Allan, G.; Bubert, C.; Smith, A.; Tutill, H.; Purohit, A.; Day, J.; Mahon, M.; Reed, M.; Potter, B. *ChemMedChem* **2006**, *1*, 464. (d) Fischer, D. S.; Woo, L. W. L.; Mahon, M. F.; Purohit, A.; Reed, M. J.; Potter, B. V. L. *Bioorg. Med. Chem.* **2003**, *11*, 1685. (e) Labrie, F. *Mol. Cell. Endocrinol.* **1991**, *78*, C113.

(f) MacCarthy-Morrogh, L.; Townsend, P. A.; Purohit, A.; Hejaz, H. A. M.; Potter, B. V. L.; Reed, M. J.; Packham, G. *Cancer Res.* **2000**, *60*, 5441. Review on enantiomeric steroids: (g) Biellmann, J. F. *Chem. Rev.* **2003**, *103*, 2019.

(40) (a) Ficini, J.; Krief, A. *Tetrahedron Lett.* **1969**, *10*, 1431. (b) Ficini, J. *Tetrahedron* **1976**, *32*, 1449.

(41) (a) Ynamides are more stable and conveniently prepared than ynamines and have recently attracted much attention in organic synthesis thanks to their extraordinarily diverse chemistry but are still rarely used in enantioselective reactions; see: (b) Evano, A.; Coste, K.; Jouvin. *Angew. Chem., Int. Ed.* **2010**, *49*, 2840–2859; (c) *Angew. Chem.* **2010**, *122*, 2902–2921. (d) DeKorver, K. A.; Li, H.; Lohse, A. G.; Hayashi, R.; Lu, Z.; Zhang, Y.; Hsung, R. P. *Chem. Rev.* **2010**, *110*, 5064.

(42) Li, H.; Hsung, R. P.; DeKorver, K. A.; Wei, Y. *Org. Lett.* **2010**, *12*, 3780.

(43) A few crystals suitable for X-ray crystallography were obtained by slow diffusion of hexane into a CD₂Cl₂ solution of racemic **7a** (obtained by hydride abstraction from **5a**). Several attempts were made to use the same protocol to isolate either racemic or enantiopure **7a** on a larger scale (50–100 mg). In all cases, only intractable oils were obtained.

(44) In fact, the X-ray structures of the *tert*-butyl analogues **5a** and **7a** indicate that little structure rearrangement occurs upon hydride abstraction from the enolato complex; see above.

(45) As the C(49)–Ru–P(1)–C(1) dihedral angle is smaller in the enone complex **7a** than in the corresponding enolato derivative **5a** because of the increased π – π interactions in the former complex (see above and Table 1), we suggest that the shielding in **7b** and **7c** may be even more efficient than indicated by the C(49)–Ru–P(1)–C(1) values available for the enolato complexes **5b** and **5c**.

(46) Prepared according to Scheme 4a–c by adding β -ketoester **3b** to **2**, followed by deprotonation with triethylamine and hydride abstraction with tritylium hexafluorophosphate without chromatographic separation. The ³¹P NMR spectra of the reaction solution taken at each step showed that the diastereoisomeric ratio remained constant at ca. 70:30.

(47) The reason for the increased enantioselectivity observed upon activation by the hydride abstraction pathway (even when the minor diastereoisomer **7c** is used as catalyst, Table 3, entry 11) is probably related to the higher purity of the catalysts obtained with this method as compared to double chloride abstraction with (Et₃O)PF₆. In fact, (Et₃O)PF₆ is a highly reactive species whose slow degradation upon storing produces traces of strong acids that may interfere with the catalytic reaction. A further advantage of hydride abstraction is that the reaction is instantaneous instead of progressing overnight, like the generation of **2** from **1** by chloride abstraction with (OEt₃)PF₆.

(48) The signal assignments have been confirmed by adding a CD₂Cl₂ solution of the reaction products (**16** or **18**) to **2** (see Supporting Information). Chemical shifts (162 MHz in CD₂Cl₂): [Ru(**16b**)(PNNP)]²⁺ δ 49.1/62.9 (major) and 47.1/61.8 (minor); [Ru(**18**)(PNNP)]²⁺ δ 43.9/59.7 (major) and 45.2/61.5 (minor).

(49) The stoichiometric reaction of **7a** with Dane's diene (**15**) reached completion in about 30 min instead of less than 15 min with **7b**. Then, addition of **6a** (1 equiv) regenerated [Ru(**6a**)(PNNP)]²⁺ (**7a**) (60%) after 30 min in CD₂Cl₂ (Table 5, entry 4), as opposed to 35% in case of the exchange of the ruthenium-bound product **16b** for **6b** (entry 1).

(50) (a) This effect should not be confused with the thermodynamic product inhibition often encountered in enzymes, in which both substrate and product bind to the catalyst (the enzyme) in rapidly established equilibria that progressively shift toward product coordination as the substrate concentration decreases; see: (b) Bisswanger, H. *Enzyme Kinetics: Principles and Methods*, 2nd ed.; Wiley: Weinheim, 2008; pp 88–119.

(51) In contrast, the optimized Diels–Alder conditions for 2,3-dimethylbutadiene (**9**) require pure CH₂Cl₂ as solvent (Table 2, entries 1 and 6).¹⁵ To understand this feature, the stoichiometric Diels–Alder reaction of **7b** was repeated with diene **9** under the same

conditions. After 15 min, only 10% of **7b** had reacted, whereas its conversion with Dane's diene (**15**) was quantitative within 15 min. Thus, in the case of 2,3-dimethylbutadiene (**9**), the reactivity of the diene is probably the limiting factor, and a coordinating cosolvent such as Et₂O decreases the Lewis acidity of the system, leading to lower yield (entries 2 and 7). The low reactivity also explains why the catalytic reaction requires an excess of 2,3-dimethylbutadiene (10 equiv) (Table 2, entries 1, 2, 6, and 7). When this amount is used in the stoichiometric reaction in pure CD₂Cl₂, 70% conversion is observed after 10 min, which shows that the excess of **9** by and large fixes the reactivity problem.

(52) (a) Corey, E. J.; Loh, T. P.; Roper, T. D.; Azimioara, M. D.; Noe, M. C. *J. Am. Chem. Soc.* **1992**, *114*, 8290. (b) Paddon-Row, M. N.; Kwan, L. C.H.; Willis, A. C.; Sherburn, M. S. *Angew. Chem., Int. Ed.* **2008**, *47*, 7013.

(53) (a) Gothelf, K. V.; Hazell, R. G.; Jørgensen, K. A. *J. Am. Chem. Soc.* **1995**, *117*, 4435. (b) Gothelf, K. V.; Jørgensen, K. A. *J. Org. Chem.* **1995**, *60*, 6847.

(54) (a) Haase, C.; Sarko, C. R.; DiMare, M. J. *Org. Chem.* **1995**, *60*, 1777. (b) Garcia, J. I.; Martinez-Merino, V.; Mayoral, J. A. *J. Org. Chem.* **1998**, *63*, 2321. (c) Corey, E. J.; Matsumura, Y. *Tetrahedron Lett.* **1991**, *32*, 6289.

(55) Seebach, D.; Dahinden, R.; Marti, R. E.; Beck, A. K.; Plattner, D. A.; Kühnle, F. N. M. *J. Org. Chem.* **1995**, *60*, 1788.

(56) Evans, D. A.; Johnson, J. S. In *Comprehensive Asymmetric Catalysis*; Jacobsen, E. N.; Pfaltz, A.; Yamamoto, H., Eds.; Springer: Heidelberg, 1999; Vol. 3, p 1211.

(57) (a) Kanemasa, S.; Oderaotoshi, Y.; Yamamoto, H.; Tanaka, J.; Wada, E.; Curran, D. R. *J. Org. Chem.* **1997**, *62*, 6454. (b) Kanemasa, S.; Oderaotoshi, Y.; Sakaguchi, S.-I.; Yamamoto, H.; Tanaka, J.; Wada, E.; Curran, D. P. *J. Am. Chem. Soc.* **1998**, *120*, 3074.

(58) Evans, D. A.; Kozlowski, M. C.; Tedrow, J. S. *Tetrahedron Lett.* **1996**, *37*, 7481.

(59) Davenport, A. J.; Davies, D. L.; Fawcett, J.; Garratt, S. A.; Lad, L.; Russell, D. R. *Chem. Commun.* **1997**, 2347.

(60) Kündig, E. P.; Bourdin, B.; Bernardinelli, G. *Angew. Chem., Int. Ed. Engl.* **1994**, *33*, 1856.

(61) As discussed in ref 17b, a PM3 model predicted no reasonable source of stereochemical induction, whereas the actual crystal structure showed a very different arrangement of the substrate/catalyst complex, which indeed featured the expected shielding of the re face of the substrate.

(62) Rickerby, J.; Vallet, M.; Bernardinelli, G.; Viton, F.; Kündig, E. P. *Chem.—Eur. J.* **2007**, *13*, 3354.

(63) (a) Carmona, D.; Cativiela, C.; Elipse, S.; Lahoz, F. J.; Lamata, M. P.; López-Ram de Vitu, M. P.; Oro, L. A.; Vega, C.; Viguri, F. *Chem. Commun.* **1997**, 2351. (b) Faller, J. W.; Patel, B. P.; Albrizzio, M. A.; Curtis, M. *Organometallics* **1999**, *18*, 3096.

(64) As indicated by elementary crystal field arguments, see ref 34, pp 399–408.

(65) (a) Basolo, F.; Pearson, R. G. *Mechanisms of Inorganic Reactions*, 3rd ed.; Wiley: New York, 1963; pp 108–111. (b) Spees, S. T.; Perumareddi, J. R.; Adamson, A. W. *J. Am. Chem. Soc.* **1968**, *90*, 6626.

(66) (a) We have discussed elsewhere the factors that affect the oxophilicity of late transition metal, see ref 9 and: (b) Schotes, C.; Ranocchiarri, M.; Mezzetti, A. *Organometallics* **2011**, *30*, 3596. Similar arguments apply for fluorophilicity; see: (c) Becker, C.; Kieltisch, I.; Broggini, D.; Mezzetti, A. *Inorg. Chem.* **2003**, *42*, 8417. (d) Mezzetti, A.; Becker, C. *Helv. Chim. Acta* **2002**, *85*, 2686.

(67) (a) According to the electroneutrality principle, the covalent character of a metal–ligand bond increases with the oxidation state of the metal, which decreases the lability of the ligand.^{67b} By analogy, we suggest that the increase of the overall charge on going from [RuCl(OR)₂(PNNP)]⁺ to the dicationic β-ketoester complex **7a** similarly contributes to the inert nature of the latter species. (b) Pauling, L. *The Nature of the Chemical Bond*, 3rd ed.; Cornell University Press: New York, 1960; pp 172–174.

(68) (a) For an overview, see ref 9. For different substituents on phosphorus, see: (b) Bonaccorsi, C.; Santoro, F.; Gischi, S.; Mezzetti, A.

Organometallics **2006**, *25*, 2002. (c) Bonaccorsi, C.; Bachmann, S.; Mezzetti, A. *Tetrahedron: Asymmetry* **2003**, *14*, 845. For variations on the backbone, see: (d) Stoop, R. M.; Bachmann, S.; Valentini, M.; Mezzetti, A. *Organometallics* **2000**, *19*, 4117. (e) Gao, J. X.; Xu, P. P.; Yi, X. D.; Yang, C. B.; Zhang, H.; Cheng, S. H.; Wan, H. L.; Tsai, K. R.; Ikariya, T. *J. Mol. Catal. A: Chem.* **1999**, *147*, 105. (f) Sui-Seng, C.; Haque, F. N.; Hadzovic, A.; Pütz, A. M.; Reuss, V.; Meyer, N.; Lough, A. J.; Zimmer-De Iulius, M.; Morris, R. H. *Inorg. Chem.* **2009**, *48*, 735. (g) Zhang, H.; Yang, C. B.; Li, Y. Y.; Donga, Z. R.; Gao, J. X.; Nakamura, H.; Murata, K.; Ikariya, T. *Chem. Commun.* **2003**, 142. (h) Masson-Szymczak, A.; Riant, O.; Gref, A.; Kagan, H. B. *J. Organomet. Chem.* **1996**, *511*, 193. (i) Song, J. H.; Cho, D. J.; Jeon, S. J.; Kim, Y.-H.; Kim, T. J.; Jeong, J. H. *Inorg. Chem.* **1999**, *38*, 893. For a macrocyclic analogue, see: (j) Ranocchiarri, M.; Mezzetti, A. *Organometallics* **2009**, *28*, 1286.